Coarse estimate of frequency offset: The coarse estimation is performed in the frequency domain after correcting the fractional part of the RFO. Equation (3) can be rewritten as $[m_l(k+4)-m_l(k+2)]-[m_l(k+2)-m_l(k)]=(-1)^{l+1}$ which shows that the subcarriers are differentially modulated so that the phase difference of the two nearest even subcarriers increases (decreases) linearly as m increases for $l=1$ ($l=2$), i.e. the curve connecting the points representing the phase differences is a straight line starting from an intercept point of y-axis which is determined by the phases of the first two subcarriers or $m_l(0)$ and $m_l(2)$. In Fig. 1, the solid line illustrates the phase difference for the first training symbol when we let $m_1(0)=0$ and $m_1(2)=1$. If frequency offset is present in the received sequence, then the solid line in Fig. 1 moves up (dashed line) or down according to the sign of the frequency offset with the slope unchanged, because the subcarriers are shifted by the offset and the intercept point determined by the phase difference of the first two even subcarriers is changed. Then the distance of the two lines is just the RFO as shown in Fig. 1. The line for the second training symbol moves in the opposite direction to the first one. The common component in phase of two symbols, which may be caused by channel or symbol timing offset, can be removed by subtracting the second phase from the first one. This is the key idea of the proposed method.

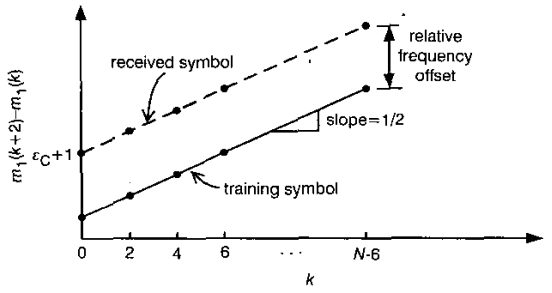

Fig. 1 *Phase difference curves for first training and received symbols*

The distance of the two lines or the estimate of the even integer offset are obtained from the following equations:

$$\hat{\epsilon}_C = \text{even\_int}\left[\frac{M}{2\pi}[\arg(P_2)-\arg(P_1)]\right] \quad (6)$$

$$P_l = \frac{2}{N}\sum_{k\in K} Y_l^*(k)Y_l((k+2)_N)C_l^*(k), \quad K \in \{0,2,\ldots,N-2\} \quad (7)$$

where even_int $[x]$ means the even integer nearest to x, $(\cdot)_N$ denotes modulo N operation, and $C_l(k)$ is defined as $C_l(k)\equiv X_l^*(k)X_l((k+2)_N)$, $k=0,1,\ldots,N-1$. $C_l(k)$ is similar to v_k used in equation (41) of [2]. However, v_k is a phase difference defined on the consecutive two OFDM symbols, while $C_l(k)$ is defined on the nearest even subcarriers in the lth symbol. We note here that to estimate the coarse frequency offset, equation (41) of [2] requires a correlation function calculated over all the possible offsets, while (7) needs only two correlation values P_1 and P_2. Therefore the computational complexity of the proposed method is much lower than that of [2]; also we know that the estimation range of the coarse estimator is $|\epsilon_C|<M$ from (6).

Simulation results: Computer simulations are given to compare the performance of the proposed algorithm (PA) and the Schmidl algorithm (SA) [2] for the AWGN channel and multipath channel examples. The impulse response of the multipath channel is $h(n)=Ae^{-n/8}e^{j\theta(n)}$, $n=0,4,\ldots,24$, where the phase $\theta(n)$ of each path is uniformly distributed over $[0,2\pi)$, and A is the normalisation factor for $\Sigma_n|h(n)|^2=1$. This amounts to a root-mean-square delay spread of 3.7 (in sample units). The symbol timing offset $\delta=3$. The parameters of the OFDM system are $N=256$ and $N_G=32$.

Fig. 2 shows the failure probability of the coarse estimator with RFO of $3M/4$ for M-PSK subcarrier modulation. It is seen that the PA shows similar performance to SA for 32-PSK modulation cases. In these cases the estimation range of the RFO is $|\epsilon_C|<32$ or a quarter of the bandwidth, and this range is sufficient for most of the practical systems with typical oscillator accuracy. According to our simulations, the variance of final estimates including the fine estimator approaches the Cramer–Rao lower bound when the failure probability of the coarse estimator is less than about 10^{-4}. Thus, as we can see in Fig. 2, the PA hardly affects the final estimate at an SNR level of over 5 dB even in the case of 64-PSK modulation. As the number of subcarriers doubled, the required SNR decreases 3 dB at the same estimation range of the RFO.

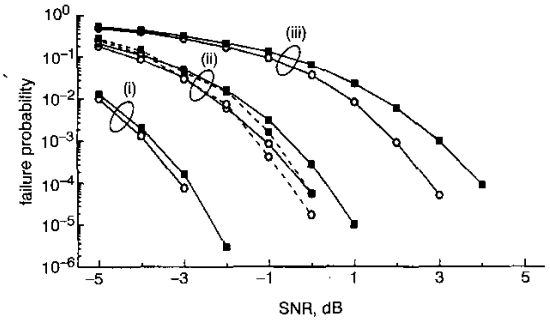

Fig. 2 *Failure probability of coarse frequency offset estimator*
(i) 16-PSK, (ii) 32-PSK, (iii) 64-PSK
■ multipath channel
○ AWGN channel
—— PA
----- SA

Conclusions: A fast algorithm is proposed for the estimation of the integer part of the RFO in the OPDM systems. Simulation results show that the performance of PA is comparable to SA with the SNRs and carrier frequency offsets of practical interest at a much lower computational complexity.

7 May 2002
Electronics Letters Online No: 20021026
DOI: 10.1049/el:20021026

Bo Seok Seo (*Research Institute for Information & Communication Technology, Korea University, Seongbook-Gu, Seoul, 136-701, Korea*)

Su Chang Kim and Jinwoo Park (*Department of Electronics Engineering, Korea University, Seongbook-Gu, Seoul, 136-701, Korea*)

References

1 MOOSE, P.H.: 'A technique for orthogonal frequency division multiplexing frequency offset correction', *IEEE Trans. Commun.*, 1994, **42**, (10), pp. 2908–2914
2 SCHMIDL, T.M., and COX, D.C.: 'Robust frequency and timing synchronization for OFDM', *IEEE Trans. Commun.*, 1997, **45**, (12), pp. 1613–1621
3 BEEK, J.J., SANDELL, M., and BORJESSON, P.O.: 'ML estimation of time and frequency offset in OFDM systems', *IEEE Trans. Signal Process.*, 1997, **45**, (7), pp. 1800–1805
4 CHUANG, J., and SOLLENBERGER, N.R.: 'Beyond 3G: wideband wireless data access based on OFDM and dynamic packet assignment', *IEEE Commun. Mag.*, 2000, **38**, (7), pp. 78–87

Generalised Sarwate bounds on periodic autocorrelations and cross-correlations of binary sequences

D.Y. Peng and P.Z. Fan

A general periodic correlation bound named generalised Sarwate bound for binary zero or low correlation zone (ZCZ/LCZ) sequence set with respect to family size, sequence length, maximum autocorrelation sidelobe, maximum cross-correlation value and the zero or low correlation zone, are derived. It is shown that all the previous periodic sequence bounds, such as Sarwate bound, Welch bound and Tang-Fan bound, are only special cases of the generalised Sarwate bound.

Introduction: For asynchronous CDMA (AS-CDMA) systems, to eliminate the multiple access interference it is necessary to design a set of spreading sequences with impulsive autocorrelation functions (ACFs) and zero cross-correlation functions (CCFs). Unfortunately, according to the Welch bound, Sarwate bound, Sidelnikov bound, Massey bound and other bounds [1–6], in theory, it is impossible to construct such an ideal set of sequences. In AS-CDMA systems, therefore, the spreading sequences are normally designed to have low autocorrelation sidelobes and low cross-correlations, such as Gold sequences, Kasami sequences, etc. To overcome the difficulty, one can consider only a specific correlation zone instead of the whole correlation range, thus resulting in the new concepts, generalised orthogonality (GO) or zero correlation zone (ZCZ), and low correlation zone (LCZ), which can be employed in quasi-synchronous CDMA (QS-CDMA) to eliminate the multiple access interference and multipath interference [7, 8]. These ideas, in fact, open a new direction in spreading sequence design.

Because the traditional bounds, such as Sarwate bound [1] and Welch bound [2], cannot directly predict the existence of the ZCZ and LCZ sequences, it is important to derive the theoretical tight limit among the sequence length n, sequence set size M, maximum autocorrelation sidelobe value ϕ_a, maximum cross-correlation value ϕ_c and low correlation zone L_{CZ} or zero correlation zone Z_{CZ}. In 2000, Tang and Fan [5] established a bound on n, M, $\phi_m = \max\{\phi_a, \phi_c\}$ and L_{CZ} (Z_{CZ}) based on Welch's technique, but including the Welch bound as a special case. In this Letter we present a more general bound, named generalised Sarwate bound due to the similar form. It is shown that all the previous periodic sequence bounds, such as the Sarwate bound, Welch bound and Tang-Fan bound, are only special cases of the generalised Sarwate bound. As for the aperiodic bound, similar results have also been obtained [6].

LCZ sequences: Let $E = \{-1, 1\}$, for any $x = (x_0, x_1, \ldots, x_{n-1})$, $y = (y_0, y_1, \ldots, y_{n-1}) \in E^n$, any integer l, the periodic correlation function $P(x, y; l)$ is defined as follows:

$$P(x, y; l) = \sum_{i=0}^{n-1} x_i y_{i+l}$$

where subscripts are reduced mod n if they exceed $n-1$ or not exceed 0, and the inner product of x and y is defined by $<x, y> = x_0y_0 + x_1y_1 + \cdots + x_{n-1}y_{n-1}$.

For $C \subseteq E^n$, $M = |C|$, $\phi_a \geq 0$, $\phi_c \geq 0$, $\phi_m = \max\{\phi_a, \phi_c\}$, the periodic low correlation zone L_{CZ}, the periodic low autocorrelation zone L_{ACZ} and the periodic low cross-correlation zone L_{CCZ} of C are defined, respectively, as follows:

$$L_{CZ} = \min\{L_{ACZ}, L_{CCZ}\},$$
$$L_{ACZ} = \max\{T \mid |P(x, x; l)| \leq \phi_a, \forall x \in C, 0 < |l| \leq T\}$$

and

$$L_{CCZ} = \max\{T \mid |P(x, y; l)| \leq \phi_c, \forall x, y \in C, x \neq y, |l| \leq T\}$$

A sequence set C with a $L_{CZ} > 0$ is called the periodic low correlation zone (LCZ) sequence set. When $\phi_m = 0$, then the LCZ sequence set becomes the periodic zero correlation zone (ZCZ) sequence set and the low correlation zone L_{CZ} becomes zero correlation zone Z_{CZ}. Tang and Fan [5] established the bounds on n, M, ϕ_m and L_{CZ} (Z_{CZ}), Peng and Fan [6] obtained aperiodic bounds on n, M, ϕ_a, ϕ_c and L_{CZ} (Z_{CZ}). In this Letter, we give periodic bounds on n, M, ϕ_a, ϕ_c and L_{CZ}.

Basic correlation properties: For any sequence $x = (x_0, x_1, \ldots, x_{n-1}) \in E^n$, any integer i, let $T^i x = (x_i, x_{i+1}, \ldots, x_{i+n-1})$, where subscripts are performed modulo n. Throughout this Letter, it is assumed that

$$w_i \geq 0, \quad i = 0, 1, \ldots, L_{cz}, \quad \sum_{i=0}^{L_{cz}} w_i = 1 \text{ and } w = (w_0, w_1, \ldots, w_{L_{cz}})$$

For $x \in E^n$, A, $B \subseteq E^n$, $|A||B| > 0$, let $W(x) = \{T^i x \mid i = 0, 1, \ldots, L_{cz}\}$, $W(A) = \cup_{x \in A} W(x)$ and

$$F(A, B) = \frac{1}{|A||B|} \sum_{x \in A} \sum_{y \in B} \sum_{s=0}^{L_{cz}} \sum_{t=0}^{L_{cz}} |<T^s x, T^t y>|^2 w_s w_t$$

Lemma 1: For any $x \in E^n$, $A \subseteq E^n$,

$$F(\{x\}, E^n) = F(A, E^n) = F(E^n, E^n) = n$$

Proof: For any x, $y \in E^n$, let $d(x, y)$ denote the Hamming distance between x and y. We have

$$\begin{aligned} F(\{x\}, E^n) &= \frac{1}{2^n} \sum_{s,t=0}^{L_{cz}} \sum_{y \in E^n} P^2(x, y, t-s) w_s w_t \\ &= \frac{1}{2^n} \sum_{s,t=0}^{L_{cz}} \sum_{y \in E^n} [n - 2d(x, T^{t-s} y)]^2 w_s w_t \\ &= \frac{1}{2^n} \sum_{s,t=0}^{L_{cz}} \sum_{y \in E^n} [n - 2d(x, y)]^2 w_s w_t \\ &= \frac{1}{2^n} \sum_{s,t=0}^{L_{cz}} \sum_{d=0}^{n} \binom{n}{d} (n-2d)^2 w_s w_t = n \end{aligned}$$

This gives the formula for $F(\{x\}, E^n)$, which does not depend on x, and thus completes the proof.

Lemma 2: For $C \subseteq E^n$, $F(C, C) \geq n$.

Proof: For any i, $j = 0, 1, \ldots, n-1$, $s = 0, 1, \ldots, L_{cz}$, define function $f(i, j, s; X)$ on $W(E^n)$ as follows. If $X = T^s x = (x_s, x_{s+1}, \ldots, x_{s+n-1}) \in W(E^n)$, where $x \in E^n$, then $f(i, j, s; X) = x_{s+i}x_{s+j}w_s$. We can verify that

$$F(A, B) = \frac{1}{|A||B|} \sum_{X \in W(A)} \sum_{Y \in W(B)} \sum_{i,j=0}^{n-1} f(i, j, s; X) f(i, j, t; Y)$$

Using the Cauchy inequality we have

$$\begin{aligned} |A||B|F(A, B) &= \left\{ \sum_{i,j=0}^{n-1} \left(\sum_{X \in W(A)} f(i, j, s; X) \right) \left(\sum_{Y \in W(B)} f(i, j, t; Y) \right) \right\}^2 \\ &\leq \sum_{i,j=0}^{n-1} \left(\sum_{X \in W(A)} f(i, j, s; X) \right)^2 \sum_{i,j=0}^{n-1} \left(\sum_{Y \in W(B)} f(i, j, t; Y) \right)^2 \\ &= |A|^2 F(A, A) |B|^2 F(B, B) \end{aligned}$$

Therefore, $|F(A, B)|^2 \leq F(A, A)F(B, B)$. Let $A = E^n$, $B = C$, we have by lemma 1

$$|F(E^n, C)|^2 \leq F(E^n, E^n)F(C, C),$$
$$F(C, C) \geq F(E^n, E^n) \geq n$$

Lemma 3: For $C \subseteq E^n$, $M = |C| > 0$, we have

$$F(C, C) \leq \frac{n^2}{M} \times \sum_{s=0}^{L_{cz}} w_s^2 + \frac{1}{M} \left(1 - \sum_{s=0}^{L_{cz}} w_s^2 \right) \phi_a^2 + \left(1 - \frac{1}{M} \right) \phi_c^2$$

Proof: We have

$$\begin{aligned} M^2 F(C, C) &= \sum_{x \in C} \sum_{s=0}^{L_{cz}} P^2(x, x, 0) w_s w_s \\ &\quad + \sum_{x \in C} \sum_{s,t=0; s \neq t}^{L_{cz}} P^2(x, x, t-s) w_s w_t \\ &\quad + \sum_{x, y \in C, x \neq y} \sum_{s,t=0}^{L_{cz}} P^2(x, y, t-s) w_s w_t \\ &\leq Mn^2 \sum_{s=0}^{L_{cz}} w_s^2 + \phi_a^2 M \sum_{s,t=0; s \neq t}^{L_{cz}} w_s w_t \\ &\quad + \phi_c^2 M(M-1) \end{aligned}$$

This completes the proof.

Bounds on periodic autocorrelation and cross-correlation of LCZ sequences: We have the following main result from lemmas 2 and 3.

Theorem: For $C \subseteq E^n$, $M = |C| > 0$, we have

$$\frac{1}{M} \left(1 - \sum_{s=0}^{L_{cz}} w_s^2 \right) \phi_a^2 + \left(1 - \frac{1}{M} \right) \phi_c^2 \geq n - \frac{n^2}{M} \sum_{s=0}^{L_{cz}} w_s^2 \qquad (1)$$

In particular, we give a lower bound of ϕ_m in the following corollary.

Corollary 1: For $C \subseteq E^n$, we have

$$\phi_m^2 \geq \frac{Mn - n^2 \sum_{s=0}^{L_{cz}} w_s^2}{M - \sum_{s=0}^{L_{cz}} w_s^2} \qquad (2)$$

For any integer $0 \le L \le Lcz$, let

$$w_s = \begin{cases} \frac{1}{L+1}, & 0 \le s \le L, \\ 0, & L < s \le L_{cz} \end{cases}$$

and $w=(w_0, w_1, \ldots, w_{L_{cz}})$, then $\sum_{s=0}^{L_{cz}} w_s^2 = 1/(L+1)$. We have by corollary 1,

Corollary 2: For $C \subseteq E^n$, any integer $0 \le L \le L_{cz}$, we have

$$\phi_m^2 \ge \frac{ML + M - n}{ML + M - 1} \tag{3}$$

In particular, let $L = L_{cz}$, we have

$$\phi_m^2 \ge \frac{ML_{cz} + M - n}{ML_{cz} + M - 1} n \tag{4}$$

which was derived by Tang-Fan [5]. If $\phi_m = 0$, we have the bound, $Z_{CZ} \le n/M - 1$, for ZCZ sequence set. In addition, we have by theorem 1,

Corollary 3: For $C \subseteq E^n$, any integer $0 \le L \le L_{cz}$,

$$\frac{1}{M}\left(1 - \frac{1}{L+1}\right)\phi_a^2 + \left(1 - \frac{1}{M}\right)\phi_c^2 \ge n - \frac{n^2}{M(L+1)} \tag{5}$$

In particular, let $L = n - 1$, we have

$$\frac{n-1}{(M-1)n^2}\phi_a^2 + \frac{1}{n}\phi_c^2 \ge 1 \tag{6}$$

which was obtained by Sarwate [1]. Further, let $\phi_m = \max\{\phi_a, \phi_c\}$, then (6) becomes

$$\phi_m^2 \ge \frac{(M-1)n^2}{Mn - 1} \tag{7}$$

which is the famous Welch bound [2].

Acknowledgments: This work was supported by the National Science Foundation of China (NSFC) under Grant No. 69931050 and 69825102, the National Key Laboratory of Communications (UESTC), Royal Society (UK), and the Millennium Project of MEXT (Japan).

5 June 2002
Electronics Letters Online No: 20021064
DOI: 10.1049/el:20021064

D.Y. Peng and P.Z. Fan (*Institute of Mobile Communications, Southwest Jiaotong University, Chengdu, Sichuan 610031, People's Republic of China*)

E-mail: daiyuan_peng@hotmail.com

References

1 SARWATE, D.V.: 'Bounds on crosscorrelation and autocorrelation of sequences', *IEEE Trans. Inf. Theory*, **25**, , 1979, pp. 720–724
2 WELCH, L.R.: 'Lower bounds on the maximum crosscorrelation of signals', *IEEE Trans. Inf. Theory*, 1974, **20**, pp. 397–399
3 SIDELNIKOV, V.M.: 'On mutual correlation of sequences', *Soviet Math Doklady*, 1971, **12**, pp. 197–201
4 MASSEY, J.L.: 'On Welch's bound for the crosscorrelation of a sequence set'. Proc. IEEE ISIT'90, San Diego, CA, USA, September 1990, p. 385
5 TANG, X.H., FAN, P.Z., and MATSUFUJI, S.: 'Lower bounds on the maximum correlation of sequence set with low or zero correlation zone', *Electron. Lett.*, 2000, **36**, (6), pp. 551–552
6 PENG, D.Y., and FAN, P.Z.: 'Lower bounds on the aperiodic correlation of LCZ and ZCZ sequences' *in* FAN, P.Z., SUEHIRO, N., and DARNELL, M. (Eds.): 'Sequence design and applications for CDMA systems' (Southwest Jiaotong University Press, 2001, ISBN 7-81057-609-7/TN.264), pp. 99–106
7 FAN, P.Z., SUEHIRO, N., KUROYANAGI, N., and DENG, X.M.: 'A class of binary sequences with zero correlation zone', *Electron. Lett.*, 1999, **35**, pp. 777–779
8 FAN, P.Z., and HAO, L.: 'Generalized orthogonal sequences and their applications in synchronous CDMA systems', *IEICE Trans. Fundament.*, 2000, **E83-A**, (11), pp. 1–16

5 inch $MgAl_2O_4$ phosphor screen for projection display

Qiong-Hua Wang, Jianbo Cheng, Zulun Lin and Gang Yang

A new kind of $MgAl_2O_4$ phosphor screen for projection display is reported. The 5 inch phosphor screen is fabricated by depositing powder on $MgAl_2O_4$ substrate. Because $MgAl_2O_4$ has the characteristics of higher heat conductivity than the conventional glass faceplate, the phosphor screen achieves very high brightness, good contrast ratio, high resolution and long lifetime, and therefore realises large-screen projection display.

Introduction: In spite of all the attention received by novel technologies such as microdisplays based on liquid crystal and micromechanical technologies, about 98% of rear-projection televisions rely on cathode ray tube (CRT) technology to create their images [1]. It is a mature technology that is reliable and relatively easy to manufacture.

CRTs have some distinct limitations however, that leave room for improvement in rear-projection displays. The tubes – including the faceplate – are made of glass. With current displays relying on 7 to 12 inch diagonal picture tubes, the front glass is thick. Glass has relatively low thermal conductivity, which in turn means that the phosphor layers must operate at a higher temperature. This is due to the fact that only a fraction of the energy from the electron beam is converted into light, and most of the remainder becomes heat. This results in phosphor saturation and degradation. As a result, the amount of light that can be generated with a glass-faced tube is limited, with a typical 9 inch projection CRT producing just 1200 lumens. The thick glass also creates problems with diffusion of the projected light, further decreasing efficiency [2].

Projection CRTs with traditional materials also require larger screens to achieve the high resolutions required for applications such as HDTV. It is more difficult to create the small beam size required for high-resolution output in smaller screens.

If rear-projection CRTs are to be bright enough and have sufficient resolution to compete with the high-brightness microdisplay projection engines, new materials will have to be used. Previously, we have reported on 2 to 3 inch projection CRTs using $Y_3Al_5O_{12}$ (YAG), which offers high luminance, high resolution, and longevity. However, YAG is a mono-crystal material that is not only expensive but it is also difficult to scale up to 5 inches [3, 4].

$MgAl_2O_4$, which we will abbreviate as M, is a multi-crystal material that holds promise for creating phosphor screens for projection CRTs with high brightness and high resolution.

In this Letter, we report on the novel 5 inch M phosphor screen's structure and fabrication, performances and applications in detail.

Structure and fabrication: The M phosphor screen's key is to use an M faceplate as the substrate for the phosphor, with phosphor powder as the cathodoluminescent material, as shown in Fig. 1. Because M is a kind of multi-crystal material, it can be easily manufactured at a low cost. The material also supports larger diameters than YAG – the diameter of M projection CRT is 5 inches, which is bigger than YAG projection CRT – yet the faceplate is much thinner than the traditional glass designs. M's coefficient of thermal conductivity is about one order of magnitude higher than that of glass: $\lambda = 0.13\ W \cdot cm^{-1} \cdot K^{-1}$ for M as compared with $\lambda = 0.01\ W \cdot cm^{-1} \cdot K^{-1}$ for glass at room temperature.

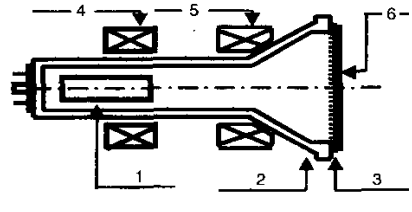

Fig. 1 *Schematic diagram of $MgAl_2O_4$ phosphor screen*
1. Electron gun 2. Glass envelope 3. Low temperature frit glass 4. Magnetic focusing yoke 5. Deflection yoke 6. M phosphor screen